heritage

MDPI

Article

Preliminary Studies of the Effects of Nanoconsolidants on Mural Paint Layers with a Lack of Cohesion

Berenice Baiza [1], Milene Gil [1], Cristina Galacho [1,2], António Candeias [1,2] and Penka I. Girginova [1,*]

1   HERCULES Laboratory, University of Évora, Palácio do Vimioso, Largo Marquês de Marialva, 8, 7000-809 Évora, Portugal; m43716@alunos.uevora.pt (B.B.); milenegil@uevora.pt (M.G.); pcg@uevora.pt (C.G.); candeias@uevora.pt (A.C.)
2   Chemistry Department of School of Sciences and Technology, University of Évora, Rua Romão Ramalho 59, 7000-671 Évora, Portugal
*   Correspondence: penka@uevora.pt

Abstract: This paper reports the preliminary results of a comparative analysis of the effects of three consolidants on the color appearance of *fresco* paint layers affected by lack of cohesion. In vitro assays were performed with a laboratory-synthesized nanolime, a commercial nanolime (CaLoSiL® IP25), and a commercial acrylic resin (Primal™ SF-016 ER®) applied by nebulization over two sets of replicas of *buon* and *lime fresco* painted with red and yellow ochres and smalt pigments. The paint layers were surveyed before, one week, and one month after treatment with technical photography in the visible range (Vis) and ultraviolet-induced fluorescence in the visible range (UVF), as well as optical microscopy (OM-Vis), colorimetry, spectrophotometry, and scanning electron microscopy coupled with energy dispersive x-ray spectroscopy (SEM-EDS). Experimental work also comprised the synthesis of nanolime and its characterization by X-ray diffraction (XRD), scanning electron microscopy (SEM), Fourier-transform infrared spectroscopy (FTIR), and thermogravimetry analysis (TGA-DTG). The results show no alteration on pigments' spectral curves and elemental composition. The increase in the CIEL* coordinate and ΔE color variation noticed after the treatment with the nanolimes is associated with a white haze formation on the paint surfaces. The impact on color appearance is higher on the darker tones.

Keywords: consolidants; frescoes; nanolime; acrylic resin; synthesis; colorimetry; OM-Vis; SEM-EDS

1. Introduction

According to the International Council on Monuments and Sites (ICOMOS), mural paintings form an integral part of the monuments and heritage sites that should be preserved in situ whenever possible [1]. Frescoes are one of the main types of mural paintings, used since antiquity till the twentieth century. What makes this technique so unique is that the pigments are laid down on damp lime-based mortar in a certain way that the pigments become fixed by the carbonatation of the calcium hydroxide contained in the underneath ground [2,3].

Fresco and *secco* mural paintings, being part of an architectural surface, are often exposed to weathering phenomena, which over time may severely affect their structure and composition [4]. The resulting degradation can vary from structural damage, aesthetic modifications, chemical and physical alterations of the paint layers, and mortar constituents [5]. Among the deterioration features commonly found in these cases is the lack of cohesion of paint layers. Lack of cohesion occurs when the pigment particles in a paint layer become exposed and gradually loose. When it manifests, the need for a consolidation treatment emerges to strengthen its crystalline network and to improve the mechanical resistances within its structure.

Consolidation of a porous material is an irreversible process. Any intervention should respect the integrity, nature, elaboration technique, and aesthetic of the decayed masterpiece

being treated [6,7]. Consolidation does not solely depend on the composition of the art object but on different factors concerning the consolidant, such as type, concentration, solvent, ambient conditions, and application technique [8,9]. An effective consolidant must improve the physicochemical properties of the *fresco* while preserving its aesthetic properties and be efficient, durable, and environmentally friendly without producing harmful by-products [1,6].

For the past sixty years, different types of products have been successfully applied but have also produced some drawbacks (e.g., vinyl and acrylic polymers, organosilicates, baryta water, and lime water) [10–13]. Acrylic and vinyl resins, for example, have a low rate of penetration that may produce a hydrophobic film that obstructs water permeability [12]. Lime water ($Ca(OH)_{2(aq)}$) is harmless on mortars, but over paint layers can form a carbonatation veil over the surface [10]. Baryte water ($Ba(OH)_{2(aq)}$) is best when applied to mural paintings affected by calcium sulfate damage. However, $Ba(OH)_{2(aq)}$ is not fully compatible with the lime-based mural painting matrix, leading to the deposition of small amounts of barium carbonate or sulfate to the calcium carbonate matrix [11]. To overcome some of these issues, the development of nanoconsolidants as an alternative to traditional consolidants has occurred over the past few decades [14–16]. Nanoconsolidants, having the advantage of nanomaterials, are expected to present improved properties and open new research topics [14,15]. Inorganic nanoconsolidants and their composites, in particular, alkali earth metals hydroxides and oxides (e.g., $Ca(OH)_2$, $Mg(OH)_2$, MgO), have become of interest for consolidation and conservation of paper [16–18], lime mortar and stone [15,16,18,19], wood [16,18,20], and earthen constructions [21]. Some of their beneficial characteristics are enhanced stability, good penetration capacity inside decayed substrates, high potential for long-term durability, and efficiency [15]. The effectiveness of nanoconsolidant dispersions particularly depends on the dimension of the particles and is undesirable and harmful for application particles that tend to agglomerate and form clusters. Particles dimensions influence the lattice symmetry, surface free energy, electronic structure, carbonatation mechanism, and together with the preparation method (for example, the use of templating agent), could influence the particles agglomeration rate.

Nanoparticles (NPs) of calcium hydroxide ($Ca(OH)_2$) dispersed in short-chain alcohols (generically named nanolime) have become a material of interest for the consolidation of frescoes due to their high compatibility, as both are lime-based materials [18]. If applied to frescoes, limestones, and lime mortars, nanolime can enhance the strength and the cohesion in the porous decayed material [10,18,22,23]. Synthesis methods of preparation of nanolime and nanolime consolidation effectiveness have already been a subject of a preview study carried out in our research group [23]. The main advantages of nanolime are the high surface area available and higher reactivity, assuring a faster carbonatation process. As a result, consistent consolidation can be expected within a time frame of seven days to one month after treatment [24]. However, several authors have concluded that nanolime's main limitation is white haze formation, markedly when applied in frescoes [25–28]. Moreover, the application of nanolime has many variables that may limit its effectiveness, such as dispersing solvent, dispersion concentration, application procedure, and environmental conditions [17,24,26,28–32].

Despite the research already undertaken in previous studies with commercial and laboratory-synthesized nanolime, there is still little research on the assessment of nanolime treatments in mural paint surfaces. To the best of our knowledge, the most recent was made by Becherini et al. [27] and Bourguignon et al. [28] in 2018 and Normand et al. [13] in 2020, which was a comparative analysis of their efficacy and compatibility and showed that nanolime dispersions (5 g/L in ethanol (applied till saturation); 20 g/L in 2-propanol) induced notable color variation seen as white haze formation in the painted surfaces. They suggest reducing white haze by applying lower concentrations of the product. They also observed that many variabilities affect the treatment, such as the painting technique and water and salt content. According to Bourguignon et al. [28], surface hardness after

treatment is dependent on the painting technique but not on the pigment. Normand et al. [13] found that water absorption of the substrate incremented after application.

In this context, the current research intends to widen the understanding of the effect of two nanolimes (laboratory prepared and commercial) and commercial acrylic resin produced on a set of frescoes paint replicas with a lack of cohesion. The main purpose was to verify the impact on color appearance suffered by the frescoes paint layers after the products were applied, using a multi-analytical setup, in an attempt to answer doubts raised by conservator-restorers. Herein we report our first preliminary results.

2. Materials and Methods

2.1. Nanolime Synthesis

$Ca(OH)_2$ NPs were synthesized by precipitation method [29,33] of equal volumes of aqueous solutions of 0.4 M calcium chloride ($CaCl_2$, 99.9% pure, Sigma-Aldrich) and 0.8 M sodium hydroxide (NaOH, 99.9% pure, Sigma-Aldrich) at T = 90 °C with the addition of Triton X-100 (5 g, t-Oct-C_6H_4-$(OCH_2CH_2)_x OH$) [23,34], according to Equation (1).

$$CaCl_{2(aq)} + 2NaOH_{(aq)} \xrightarrow{\Delta\ 90\ °C,\ H_2O,\ Triton\ X-100} Ca(OH)_{2(s)} + 2NaCl_{(aq)} \tag{1}$$

The reaction took place for one hour after the dropwise addition of hot NaOH solution was completed. The obtained white precipitate of $Ca(OH)_2$ NPs and supernatant were cooled down to room temperature under normal atmosphere and washed with Milli Q water with consecutive cycles of agitation (vortex)/sonication (US bath)/centrifugation/ decantation until the by-product of the reaction, sodium chloride (NaCl), was removed. Silver nitrate test (0.1 M $AgNO_3$) confirmed the presence or absence of chloride anions. Once the white precipitate of silver chloride (AgCl) was not observable, Milli Q water was substituted by ethanol for the last cycle wash, followed by a drying process at a temperature of 70 °C.

2.2. Fresco Replicas Preparation

Sixty replicas of paint layers with lack of cohesion (dimensions 5 × 5 × 5 cm) were made in *buon fresco* and lime *fresco* painting techniques with red and yellow ochres and smalt pigments from *Kremer pigmente* (Aichstette, Germany). Ochres are among the most common pigments used worldwide in both painting techniques. Smalt pigment was of particular interest for future conservation purposes as it was present in 16–17 c. Portuguese frescoes, show a lack of cohesion and different signs of physical and chemical deterioration [35].

The paint replicas were made in vitro at ambient conditions (T = 22 °C and RH = 59%). The rendering of the fresco replicas consisted of two layers of lime-based mortars. The inner layer of *arriccio* was of coarser siliceous-based aggregates, while the superficial layer, called *intonaco*, was of finer calcium-based aggregates. The composition of the two mortar layers and the ratio of lime/aggregates by volume is presented in Table 1.

Table 1. Composition of the mortar layers of the replicas (parts by volume).

Ariccio	Intonaco
1 part hydrated lime putty; 2 parts siliceous sand;	1 part hydrated lime putty; 2 part cream of marble;

The preparation of the paint layers for the *buon fresco* (pigments + water) and the lime *fresco* (pigments + lime milk) is in Table 2. Two sets of twelve replicas for each pictorial technique were made, except for smalt, which was only prepared in lime *fresco*. To assure the deterioration by lack of cohesion, pigment content was oversaturated. Later, the paint mixtures were laid over the fresh *intonaco* with three thick brush strokes.

Table 2. Composition of the paint layers of buon and lime fresco replicas (BF—buon fresco; LF—lime fresco; r—red; y—yellow; b—blue).

Buon fresco paint layer	
rBF	**yBF**
4 g red ochre pigment (Kremer French Ochre RTFLES-40020®, Kremer pigmente, Aichstetten, Germany); 10 mL tap water;	4 g yellow ochre pigment (Kremer French Ochre JCLES-40040®, Kremer pigmente, Aichstetten, Germany); 10 mL tap water;

Lime *fresco* paint layer		
rLF	**yLF**	**bLF**
5 g red ochre pigment (Kremer French Ochre RTFLES-40020®) 4 pp of milk lime	5 g yellow ochre pigment (Kremer French Ochre JCLES -40040®) 4 pp of milk lime	5 g of smalt pigment (Kremer Smalt-10010®, Kremer pigmente, Aichstetten, Germany) 4 pp of milk lime

After laying down the paint layers, the *fresco* sets remained to dry in the laboratory under ambient conditions (T = 22 ± 2 °C, RH = 57 ± 9%) for a month.

2.3. Consolidants Application

The consolidants were applied as described in Table 3. They were applied to the replica surfaces five consecutive times by nebulization at a distance circa 5 cm under ambient conditions: T = 23 °C, RH = 50% (laboratory-synthesized nanolime), and T = 21 °C, RH = 46% (CaLoSiL® IP25 and Primal®). Consolidant application via nebulization was preferred over brush in order to prevent possible dragging of parts of the paint layer of *fresco* with loss of cohesion due to brush intervention. In addition, this preferred technique could also allow us to limit the amount of dispersion applied to the substrate and ensure better control of the uniformity of the consolidant product over the surface.

Table 3. Consolidants tested on the *fresco* replicas.

Name	Chemical Composition/Manufacturer
LAB nanolime	Dispersion of $Ca(OH)_2$ NPs, 25 g/L in Acetone:Ethanol (1:10). Size (SEM): between 18–713 nm
CaLoSiL® IP25	Dispersion of $Ca(OH)_2$ NPs, 25 g/L in iso-propanol (IBZ Salzchemie GmbH & Co. KG, Halsbruecke, Germany) Applied as acquired. Size: between 50–250 nm (Technical Datasheet)
Primal™ SF-016 ER®	Acrylic polymer dispersion (Dow Coating Materials, United States of America): 50–51% solid content. Applied diluted at 2% in tap water, which is a common concentration used in past conservation works [12].

The total number of treated samples was forty-five: three replicas for each pigment/painting technique/consolidant. Upon completion, the paint replicas were kept under ambient conditions (T = 24 ± 3 °C, RH = 50 ± 4%).

2.4. Instrumentation

2.4.1. Nanolime Characterization

Commercial and laboratory-synthesized nanolime were characterized by X-Ray Diffraction (XRD), Scanning Electron Microscopy (SEM), Fourier-transform infrared spectroscopy (FTIR), and Thermogravimetry Analysis (TGA-DTG).

The identification of crystalline phases of the dried NPs was performed with a BRUKER AXS D8 Discovery XRD with monochromatized Cu Kα radiation k = 1.5406 Å operating at 40 kV and 40 mA in the 2θ range 3–75° with a step size of 0.05° (2θ) and 1 s per step (increment: 0.05°, time 1000 s, steps = 1438). The DIFRAC.SUITE.EVA software identified the mineral phases with Powder Diffraction Files of the International Center for Diffraction Data-2.

SEM analyses were performed on a variable pressure scanning electron microscope HITACHI S-3700N coupled with an energy dispersive X-ray spectrometer BRUKER XFlash 5010 SDD EDS. For SEM analysis, diluted nanolime dispersions in 2-propanol were deposited over a glass plate and coated with a metallic conductive layer of gold/palladium with Quantum Q5150RES/sputter coater SC 7620 Polaron.

FTIR spectroscopy of KBr pellets (FTIR grade) was recorded on a BRUKER Hyperion 3000 spectrophotometer with OPUS 7.2 software in the range of 400–4000 cm^{-1} with a resolution of 4 cm^{-1}.

TGA-DTG analyses were performed with a Simultaneous Thermal Analyzer STA NETZSCH 449 F3 Jupiter under an inert atmosphere of Nitrogen (Air Liquid Alpha gas compressed N$_2$) with a flow rate of 70 mL/min, in a temperature range of 10 °C–1000 °C and a heating rate of 10 °C/min.

2.4.2. Treatment Evaluation

The paint layers were documented before and after treatment by:

(a) Technical photography with visible (Vis) and ultraviolet-induced visible fluorescence (UVF) captured with a Canon EOS 800D 24 Mpx. Vis was shot in daylight; for UVF, a XeLED-Ni3UV-R4-365 (120-250VAC) input was used;

(b) Optical microscopy (OM-Vis) performed with a stereozoom microscope Leica M205C at 7.8× magnification coupled with a Nikon DS-Fil digital camera;

(c) Colorimetry and spectrophotometry measured with a Data Color Check Plus II, in SCE and Standard Illuminant/Observer D65/10°, and aperture size USAV (⌀ 25 mm). Three replicas of the same pigment/paint technique were measured for each product before, one week and one month after consolidation. The results obtained in CIEL*a*b* chromatic space are the average of three measurements (three light flashes) taken on each of the replicas paint layers in an area of 2.5 cm in diameter (Figure 1). Total color variations (ΔE*) and absolute color difference (ΔH) were calculated according to Equations (2) and (3), respectively [36].

$$\Delta E_{ab}^* = \left((\Delta L^*)^2 + (\Delta a^*)^2 + (\Delta b^*)^2 \right)^{1/2} \tag{2}$$

Δ*L**, Δ*a**, and Δ*b** correspond to variations in the color values in the dark–light, red–green, and yellow–blue axes.

$$\Delta H_{ab}^* = \left[(\Delta E_{ab}^*)^2 - (\Delta L_{ab}^*)^2 - (\Delta C)^2 \right]^{1/2} \tag{3}$$

where chroma difference Δ*C** values were taken by the colorimetry software.

(d) Painted surfaces were analyzed before and after treatment (one week and one month) by SEM-EDS. SEM imaging was completed in backscattered electron (BSE) mode. EDS analysis and quantification were acquired with Esprit 1.9 software from Brüker corporation.
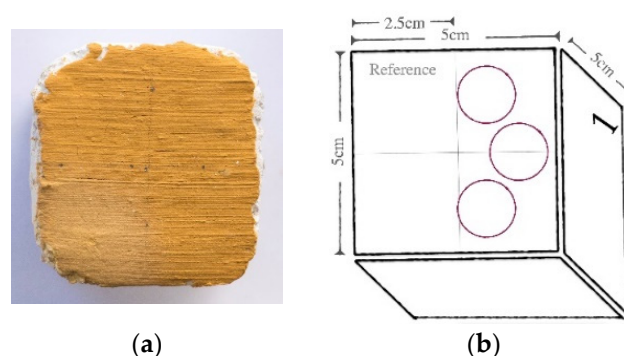
(**a**)   (**b**)

Figure 1. Colorimetry and spectrophotometry: analyzed areas. The results obtained in CIEL*a*b* chromatic space are the average of three measurements (three points and three light flashes) taken on each of the replica's paint layers in an area of 2.5 cm in diameter. (**a**) Real sample surface; (**b**) Schematic representation of the analyzed surfaces.

Two-way ANOVA followed by Bonferroni's multiple comparisons test statistical analysis was performed with the ΔE^* parameter using the software GraphPadPrism 7.00. Differences with a *p*-value ≥ 0.05 were considered statistically significant.

3. Results and Discussion

3.1. Characterization of the Laboratory-Synthesized Nanolime (LAB Nanolime)

The powder XRD pattern of LAB nanolime (Figure 2a) shows the characteristic peaks of the main crystalline phase of $Ca(OH)_2$ (calcium hydroxide) and the presence of low-intensity peaks of the crystalline phase of $CaCO_3$ (calcium carbonate). The presence of $CaCO_3$ indicates a partial carbonatation of LAB nanolime by atmospheric carbon dioxide (CO_2) and humidity when exposed to air during the drying process [37] and analysis. The characteristic hexagonal shape of the $Ca(OH)_2$ was shown by SEM analysis (Figures 2b and A1, Appendix A). Two groups of distinct particles dimensions were observed: a large number of NPs of diameter <100 nm and clusters of larger particles of diameter >100 nm (Figure A2, Appendix A). The former NPs display a mean diameter of 47 nm (observed d_{min} of 18 nm and d_{max} of 83), and the later particles show a mean diameter of 300 nm (observed d_{min} of 165 nm and d_{max} of 592 nm) and less uniform orientation compared to the smallest NPs.

The infrared spectra (Figure 2c) of the synthesized $Ca(OH)_2$ NPs confirms the presence of $Ca(OH)_2$. The presence of the bands at wavelengths 3640 cm^{-1} (s), 3446 cm^{-1} (w), and 1600 cm^{-1} (w) correspond to the stretching of O-H and H-O-H [38], while the bands present at 2892 cm^{-1} (w), 2338 cm^{-1} (w), 1459 cm^{-1} (m), and 870 cm^{-1} (w) suggest the formation of $CaCO_3$. Surfactant characteristic bands [39] were not found.

The TGA-DTG curve (Figure 2d) presents two temperature ranges: 350–550 °C and 600–850 °C, where significant weight loss occurred, determining the decomposition of $Ca(OH)_2$ and $CaCO_3$, respectively [40,41]. The average percentage of calcite was 33%, signifying the amount of nanolime that carbonated at any stage: synthesis, drying, and storage. TGA-DTG analysis confirms the absence of surfactant.
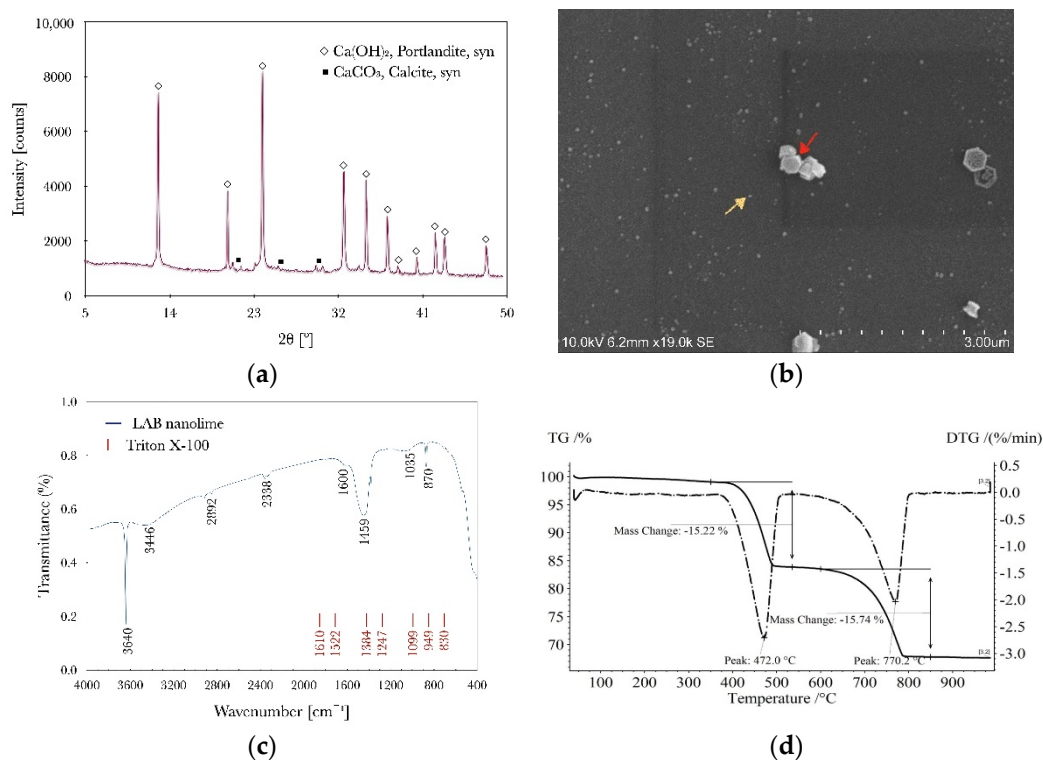
Figure 2. Characterization of LAB nanoparticles: (**a**) XRD pattern; (**b**) SEM image (yellow arrow—NPs < 100 nm; red arrow—NPs > 100 nm); (**c**) FT-IR spectra (red: characteristic peaks of Triton X-100 [39]); (**d**) TGA-DTG curves.

3.2. Evaluation of Treatment

The next sections' discussions on the effects of the consolidants on the color appearance in the paint layers of the replicas have been based on the preliminary data obtained by colorimetry and optical and electron microscopy.

3.2.1. Optical Microscopy and Colorimetry Analysis

Figure 3 shows details of OM-Vis and the spectral curves of four paint layers made with *buon* and lime *fresco* after one week of treatment with two nanolimes. Figure 4 displays the average overall color difference ΔE* for all the replicas after one week and one month.

From Figure 3a–c, a white haze is observable over the paint layers after consolidation with the nanolimes. The visual impact is more noticeable in the darker tones of red (Figure 3). With the LAB nanolime, the white haze appears as spots spread unevenly with different sizes and shapes, while CaLoSiL® produced a more translucid pinkish veil over the surface (Figure 3a,b).

Color changes in consolidation treatments of paint layers are of particular importance, as they can alter the entire visual perception of a painting [42,43]. In the field of conservation, ΔE* ≥ 5 is an acceptable threshold for the impact on the color change that a consolidant may produce on the substrate color [27,28,42,43]. Red paint layers treated with the nanolimes LAB nanolime and CaLoSiL® showed ΔE* ≥ 5 even one month after treatment (Figure 4 and Table A1 in Appendix B). However, the shape of the spectral curves of the red ochres is not affected. Only a slight increase in the R% is noticed (Figure 3a,b).

By OM in the yellow paint layers of Figure 3c, a white haze is also perceived as translucid white spots, but the lighter hues of the pigment mask the effect reflected in lower values of ΔE*.
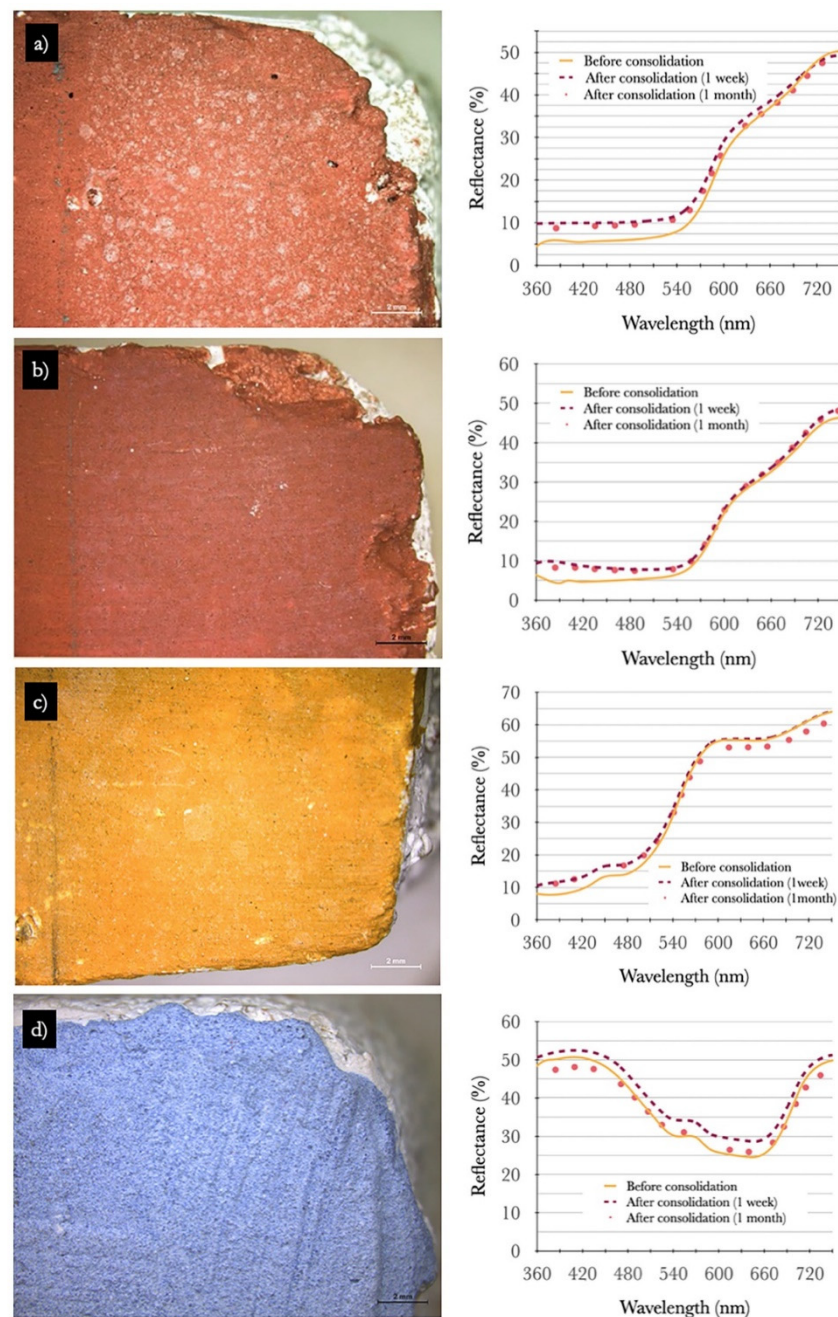
Figure 3. OM images (at 7.8× magnification) and reflectance spectral curve of paint layers consolidated with nanolimes: (**a**) rBF, LAB nanolime; (**b**) rBF, CaLoSiL®; (**c**) yBF, LAB nanolime; (**d**) bLF, LAB nanolime.

In turn, in the blue paint layers, the consolidation with the two nanolimes did not induce changes in the visual color perception, which could be explained by the low hiding power of smalt coarse particles in a white calcium matrix (Figures 3d and 5). As Figure 4 shows, ΔE < 3 is significantly lower than the ΔE* obtained for the red and yellow ochre paint layers made with *buon* and lime *fresco* (Figures 3d and 4).

Values of ΔH (shown in Table A1 in Appendix B) hint at the slight color variation for almost all paint layers, except for the red ochre paint layers, in particular treated with the commercial nanolime (applied in high concentration), where the values ΔH were higher than 2.5.
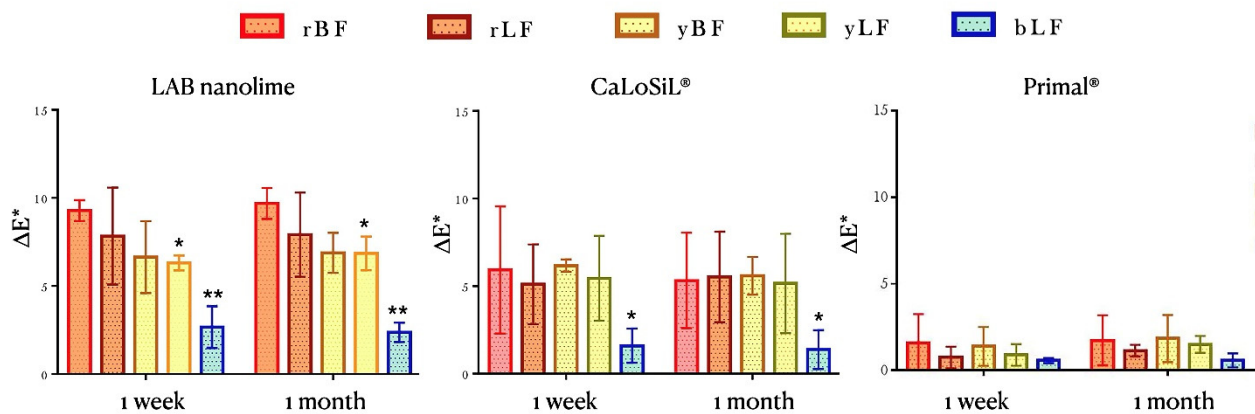
Figure 4. Average overall color difference for all the replicas (pigment/technique) at one week and one month after treatment, analyzed by ANOVA followed by Bonferroni's multiple comparisons test. In LAB nanolime: * $p < 0.05$ compared to the rBF replica; ** $p < 0.001$ compared to ochre pigments. In CaLoSiL® * $p < 0.001$ compared to the ochre pigments. The means (average) and standard deviations of the ΔE^* values are shown. Values of ΔL^*, ΔE^*, and ΔH^* are shown in Table A1, Appendix B.
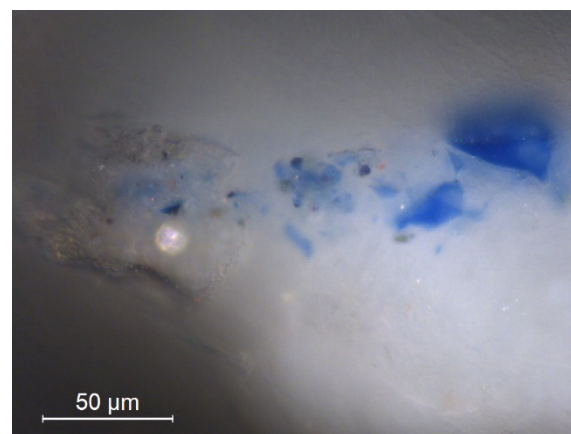

Figure 5. OM-Vis of cross-section of a blue paint layer made with lime fresco technique at $500\times$ magnification.

The finer particles of the ochre paint layers are intimately related to the increased hiding power and tinting strength of the red and yellow paint layers. This explains why these paint layers are more prone to color differences after treatment, in agreement with previous studies by Becherini et al. [27].

With nanolime treatments, ΔE^* followed the next order: ΔE^* rBF $\geq \Delta E^*$ rLF $\geq \Delta E^*$ yLF $\geq \Delta E^*$ yBF > ΔE^* bLF (Figure 4). Besides particle sizes and pigment reflective index, the painting techniques also influence the end outcomes. With the *buon fresco* technique, the pigments are only mixed with water, while on lime *fresco,* the pigments are previously combined with lime milk before being laid down on the surface of fresh mortar. The thickness of the dry paint layers is significantly higher in the second case by the amount of calcium carbonate in the composition. The pigments are more distributed in the calcium matrices and tend to enlighten, justifying right from the start the increase of L* and decrease of color coordinates +a* and +b* (Figure 5).

The mural set consolidated with the commercial acrylic resin Primal^TM SF-016 ER®, an improved version of Primal AC33 commonly used in the past as a consolidant/adhesive on mural paint layers, shows $\Delta E^* < 3$ for all the paint layers one week and one month after consolidation (Figure 4), where no visual color differences were noticeable on the paint surfaces (Figure 6). Based on the SEM-EDS analysis—discussed next in Section 3.2.2—the

explanation relies on the chemical and morphological differences between the products and how they act as consolidants.
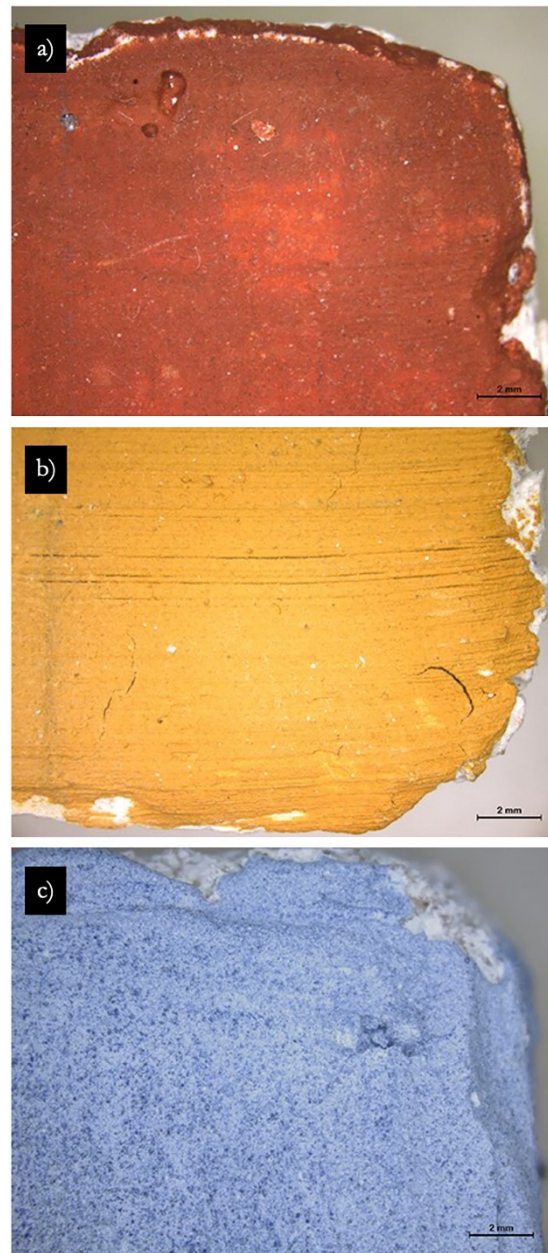

Figure 6. OM images (at 7.8× magnification) of paint layers consolidated with Primal™ SF-016 ER®: (**a**) rBF; (**b**) yLF; (**c**) bLF.

3.2.2. Scanning Electron Microscopy Analysis

Figure 7 shows SEM BSE images of a blue paint layer before and one week after treatment with two nanolimes.
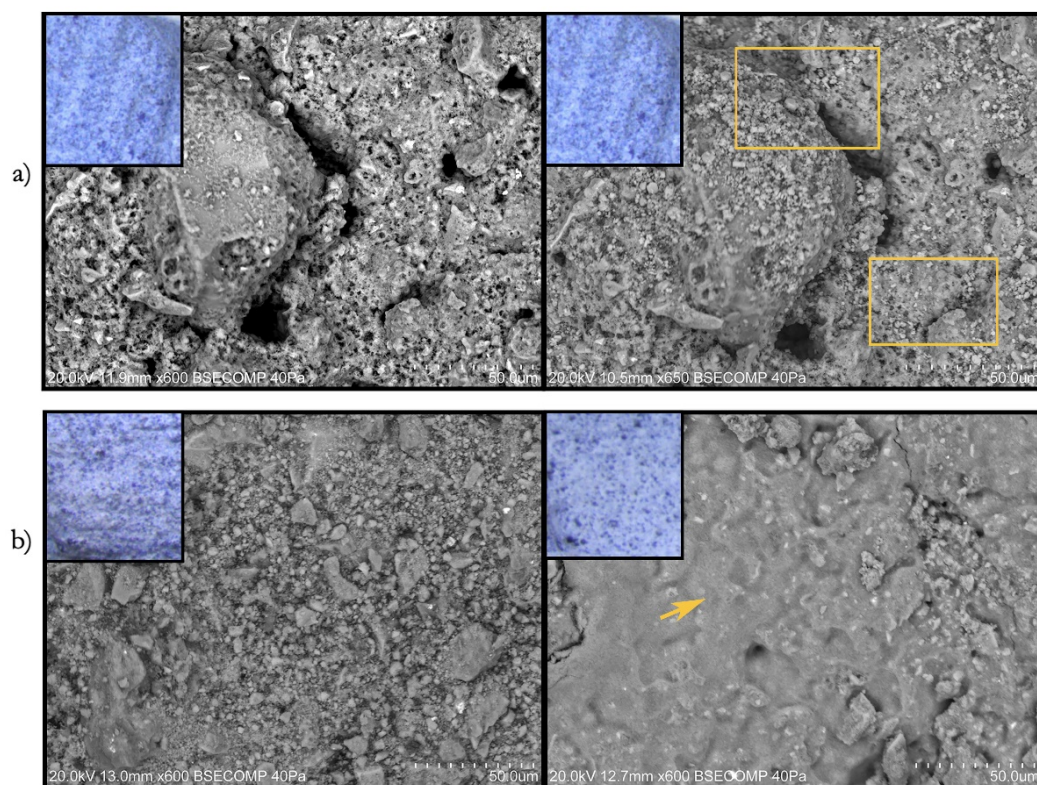
Figure 7. SEM images of LF blue paint layer before (**left**) and one week after consolidation (**right**) with (**a**) LAB nanolime; (**b**) CaLoSiL®. Detailed images obtained by OM-Vis of the studied areas are in the top left corner. Yellow rectangles enclose areas where the pores and cracks have been partially filled; yellow arrow shows the observed layer.

The surface of the replicas treated with LAB nanolime showed hexagonal-shaped particles of sizes ranging from 1.67 to 3.2 μm spread over the paint layers after one week of treatment (Figure 7a), with the same shape but bigger size than those of the synthesized nanolime (Figure 2b). Instead of penetrating in the lime mortar replica network or forming a layer, they appear heterogeneously accumulated on the paint layers, isolated and in clusters (Figure 7a), similarly to other studies on different lime-based substrates, such as carbonated stone buildings [43], limestone [44], and earthen walls [45]. A similar distribution of LAB nanolime was observable in the red and yellow paint layers (Figure A3, Appendix B). The distribution of the NPs in the painted surface in clusters appears to be a probable reason for the spotted appearance of the white haze in the red and yellow paint layers treated with LAB nanolime (Figure 3a,c).

Alternately, treatment with CaLoSiL® has led to the formation of a layer with a homogenous appearance on the red, yellow, and blue painted surfaces after one week of treatment (Figures 7b and 8), and suggests that CaLoSiL® or at least part of it accumulated on the surface, creating a coating layer. According to Ševčík et al. [46], this homogeneous layer indicates a more compacted microstructure and that nanolime has carbonatated. A similar homogeneous layer was observed by Gherardi et al. [47] after applying CaLoSiL® on limestone. At the same time, CaLoSiL® application changes the texture of the painted surfaces as is shown in Figures 7b and 8; Dei and Salvadori [48] observed the same behavior, describing it as an indication of the strengthening and re-cohesion of the paint layers.
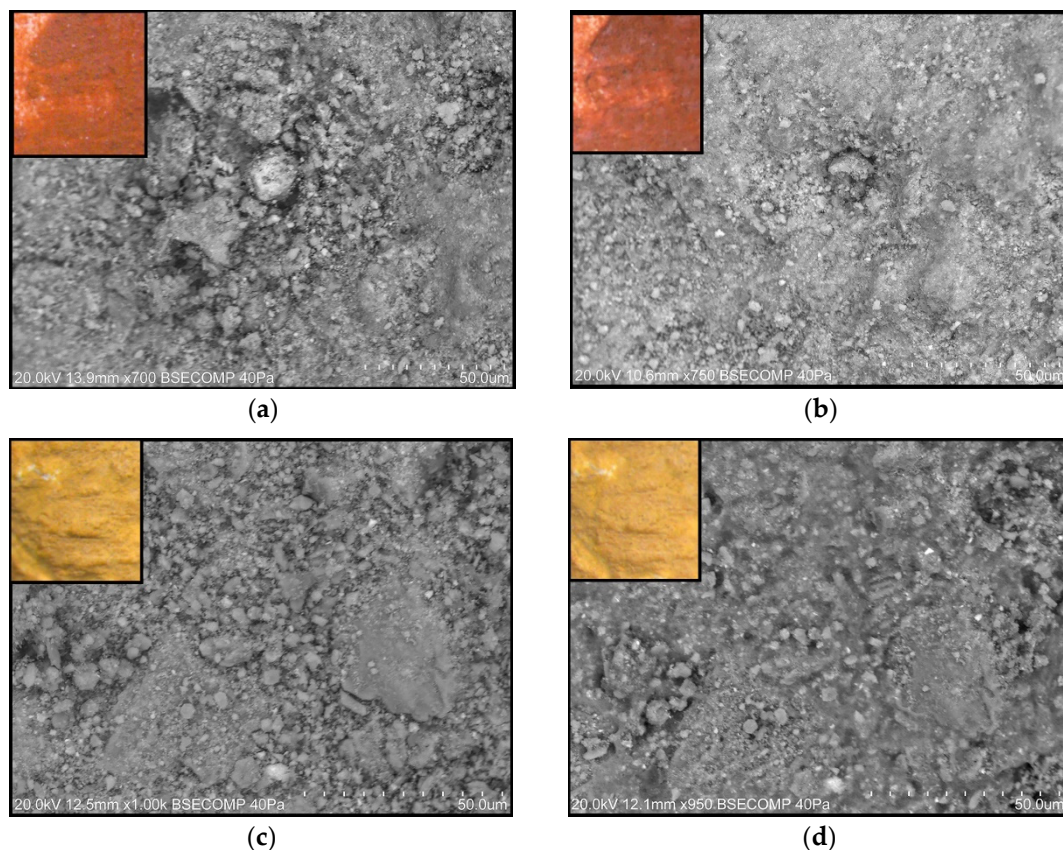
Figure 8. SEM images of red and yellow paint layers treated with CaLoSiL® before, and one week after treatment. (**a**) Red paint layer rBF before treatment; (**b**) Red paint layer rBF one week after treatment; (**c**) Yellow paint layer yLF before treatment; (**d**) Yellow paint layer yLF one week after treatment. Detailed images obtained by OM-Vis of the studied areas are in the top left corner. ((**a**,**b**)—the same area before and after treatment; (**c**,**d**)—the same area before and after treatment).

In Figure 7b, the blue-painted surface treated with CaLoSiL® appears completely covered after one week of treatment, whereas, in the ochre paint layers, some cracks and pores are incompletely covered (Figure 8). These could be because the coarser pigment particles and higher porosity of the blue paint layers permitted a higher deposition of the Ca(OH)$_2$ NPs within the substrate matrix. However, not all NPs penetrated the matrix, as the covering layer observed in the surface indicates that particles at the surface carbonatated.

Although SEM analysis showed morphological change for the two nanolimes, it is hard to conclude that it is white haze, as changes also appeared on the blue-painted surface, where the effect was not observed by OM and spectrophotometry ((Figures 3d, 4 and 7).

The two nanolimes appear to have the potential to recuperate the physicochemical network of the fresco replicas. However, these changes seem to be faster in the case of the commercial nanolime, which has carbonatated quicker than the synthesized nanolime. The difference between the nanolimes characteristics (particle size, degree of particles agglomeration, and dispersing solvent) influenced their reactivity, penetration degrees, and carbonatation mechanisms. When applied, the smaller-sized nanolime, CaLoSiL® (Table 3), carbonated more quickly. Consequently, the nanolimes had a different effect on the morphological of the paint layers. Therefore, the mechanism of the white haze formation caused by the two nanolimes might be different for each case: the accumulation of Ca(OH)$_2$ NPs on the surface (LAB nanolime) and the superficial carbonatation of the product (CaLoSiL®), as proposed by Normand et al. [13]. Control over the CaCO$_3$ polymorphs during carbonatation of NPs [46] and the speed of carbonatation through relative humidity [24] could be the key to limit the white haze formation [46]. The use of

diluted dispersions (0.05 to 5 g/L) [29–31,48] or using mixed dispersing solvents [9] can also control white haze appearance.

Another route to tackle white haze formation could be by studying the application method [26,49] or mechanical cleaning [49]. During research on the restriction of white haze formation during and after application of nanolime, it is possible to reduce the formed white haze by wetting the surface with water after application; however, do not eliminate it [26]. As an alternative, the removal of the excess nanoconsolidant after each application was the best course of action to avoid, to a large extent, the appearance of the white haze without a decrease in the consolidation effectiveness [49].

Treatment with Primal™ SF-016 ER® produced few changes in the appearance of the blue paint layers. OM images and colorimetry results confirmed results. After one week of treatment, a thin film formed in some cracks surrounding the pigment particles (Figure 9). The UVF photographic documentation and the elemental map of carbon (C) shown in Figures 10 and 11 support that the treatment with PrimalTM SF-016 ER® did not form any organic coating layer on the surface.

Figures 7 and 9 show that the treatment with nanolime compounds caused more noticeable changes in the paint layers than Primal™ SF-016 ER®. It is relevant to note that the concentration of the Primal® (2% of *v/v* of a commercial solution that contains 50–51% solid content) is lower than the concentration of LAB nanolime and CaLoSiL®, which was 25 g/L.
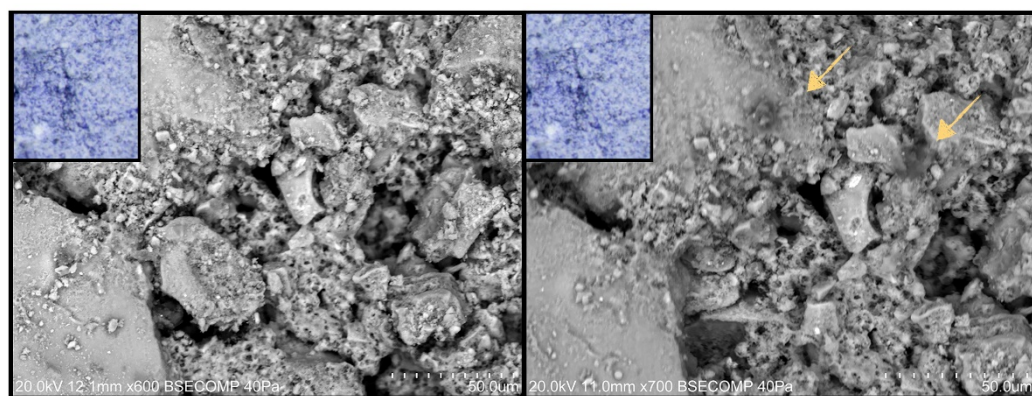

Figure 9. SEM image of an LF blue paint layer before (**left**) and one week (**right**) after consolidation with Primal™ SF-016 ER®. Yellow arrow shows the observed thin film.
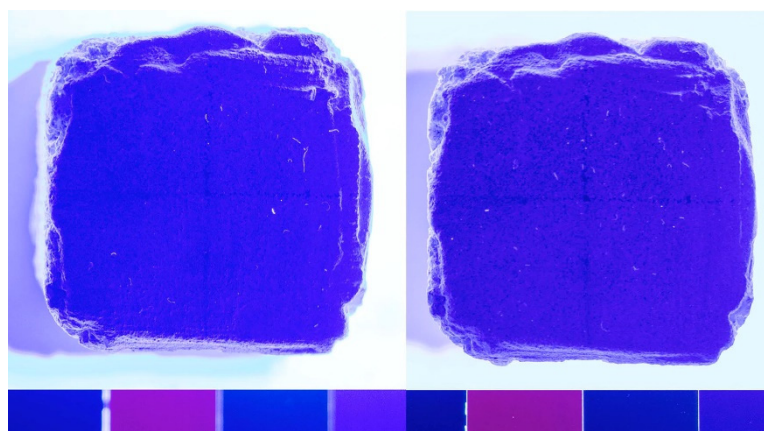

Figure 10. UV photographic documentation of the blue replica studied.

Yet, higher concentrations of Primal™ SF-016 ER® can lead to the formation of a film over the surface, which can cause the loss of the readability and integrity of the artwork in the long term, especially when exposed to aggressive environmental conditions [12,27].

Consequently, the usage of low concentrations of acrylic resins is preferred, as it can promote the penetration of the acrylic resin within the substrate and control the hydrophobic film formation.
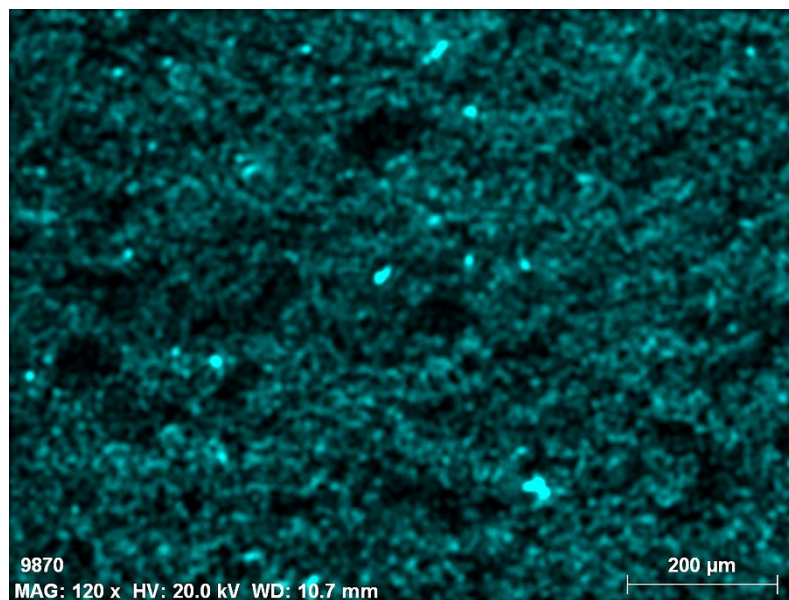

Figure 11. SEM-EDS elemental map of C of the surface area studied under SEM.

4. Conclusions

The evaluation of three consolidant revealed that the color changes followed the order: LAB nanolime > CaLoSiL® IP25 > Primal™ SF-016 ER®.

The increase of the CIEL* coordinate and ΔE color noticed with the two nanolimes after treatment is associated with a white haze formation. The impact on color appearance is higher in the darker tones. It was also dependent on the pigment. Ochre paint layers were more prone to differences in color perception after treatment with nanolime.

The obtained preliminary data open up perspectives for further studies on understating the effect of different nanoconsolidants on deteriorated *frescoes*, in particular, the effect of nanolime dispersions on the white haze formation over the paint layer and for a larger time scale. From a materials science point of view, there is a set of several factors to be explored, such as synthesis approaches to tailor particle morphology, and to avoid high agglomeration, uniform particle orientation in addition to particle kinetic stability, nature of dispersing media and dispersions concertation, and numbers of application. Assessment of the cohesion and consolidation characteristics of the treated surfaces, carbonatation mechanism, and interrelation with the nanoconsolidant nature is another further challenge. Conservation science demands consistent and various studies of the origin of white haze formation, such as, for instance, the possible relation between the distinct textures (smooth or coarse) of the paint layer surface, nanoparticles arrangement over the treated surface, and veil formation. We anticipate that this preliminary research could be extended for synthetic pigments, with potential for modern wall painting conservation.

Author Contributions: Conceptualization, M.G., C.G., A.C. and P.I.G.; methodology, B.B., M.G., C.G. and P.I.G.; validation, B.B., M.G., C.G. and P.I.G.; formal analysis, B.B., M.G., C.G. and P.I.G.; investigation, B.B., M.G., C.G. and P.I.G.; resources, M.G., C.G., A.C. and P.I.G.; writing—original draft preparation, B.B., M.G., C.G. and P.I.G.; writing—review and editing, B.B., M.G., C.G., A.C. and P.I.G.; supervision, M.G., C.G. and P.I.G.; project administration, M.G., C.G. and P.I.G.; funding acquisition, M.G., C.G., A.C. and P.I.G. All authors have read and agreed to the published version of the manuscript.

Appendix A. Laboratory-Synthesized Nanolime Characterization.

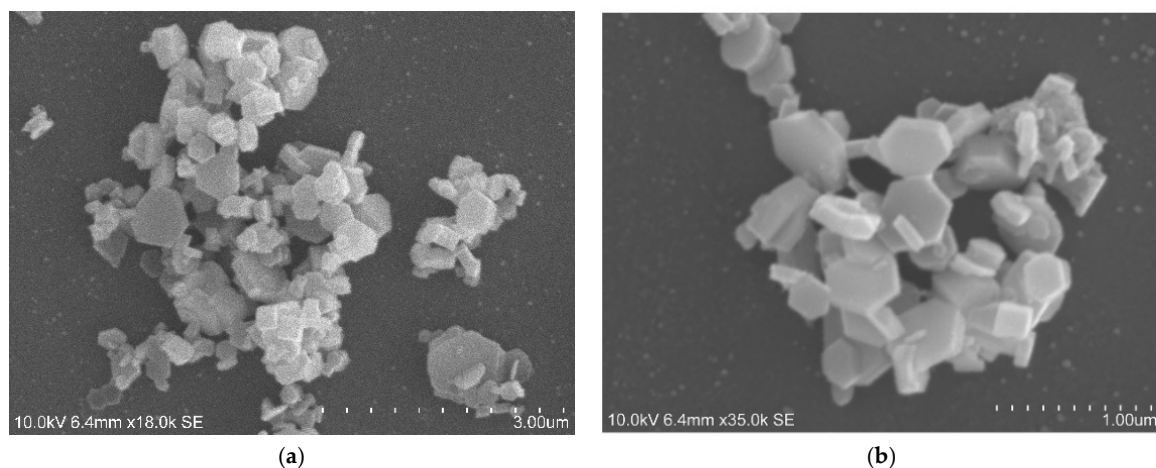(**a**)   (**b**)

Figure A1. Characterization of LAB nanoparticles: SEM images. (**a**) Magnification 18.0 k. (**b**) Magnification 35.0 k.
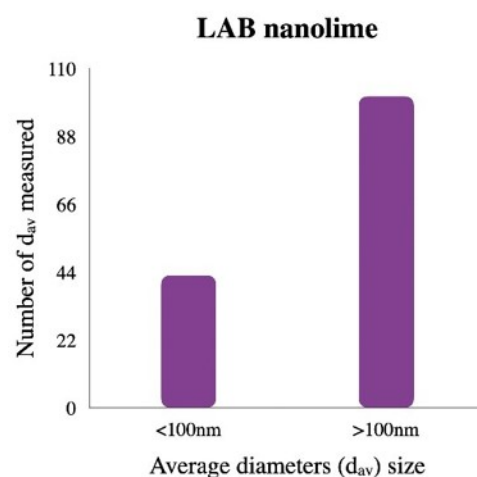

Figure A2. Particles size diagram for lab nanolime; particles dimensions taken from SEM images. Presentation is rather schematic because, while the shape of the particles is uniform, particle dimensions vary.

Appendix B. Treatment Evaluation

Table A1. Color differences using CIE*L*a*b* coordinates for the paint layers treated with the two kinds of nanolime-Lab nanolime and commercial CaLoSiL® IP25 (measurements taken one week and one month after replicas treatment). ΔL* corresponds to variations in the color values in the dark–light axis; ΔE*—total color variations and ΔH—absolute color differences were calculated according to Equations (2) and (3), respectively [37].

| Consolidant	Sample Ref.	Color	Painting Technique	ΔL*	ΔE*	ΔH*	ΔL*	ΔE*	ΔH*
				One week after			One month after		
LAB nanolime	3rBF	Red	Buon Fresco	4.48	9.91	2.5	5.05	9.10	2.21
	7rBF	Red	Buon Fresco	3.76	8.73	1.76	5.28	10.77	2.47
	11rBF	Red	Buon Fresco	4.99	9.21	1.84	3.49	9.28	2.26
	3rLF	Red	Lime Fresco	2.49	10.48	2.8	2.17	10.17	2.89
	7rLF	Red	Lime Fresco	3.64	8.53	2.06	3.14	8.44	2.10
	11rLF	Red	Lime Fresco	3.32	5.00	1.15	3.09	5.31	1.10
	4yBF	Yellow	Buon Fresco	0.66	8.99	1.55	1.52	8.14	2.14
	7yBF	Yellow	Buon Fresco	0.51	5.36	1.92	1.20	5.91	1.87
	11yBF	Yellow	Buon Fresco	−0.75	5.58	0.61	−0.94	6.62	0.39
	1yLF	Yellow	Lime Fresco	0.33	5.97	0.91	−0.15	5.81	0.89
	7yLF	Yellow	Lime Fresco	1.11	6.20	1.15	−0.06	7.69	1.19
	11yLF	Yellow	Lime Fresco	0.72	6.79	1.15	−0.48	7.06	1.10
	3bLF	Blue	Lime Fresco	−0.31	1.75	0.09	1.29	1.83	0.07
	7bLF	Blue	Lime Fresco	2.04	2.25	0.01	1.73	2.42	0.24
	12bLF	Blue	Lime Fresco	3.02	4.00	0.26	0.44	2.89	0.32
CaLoSiL® IP25	12rBF	Red	Buon Fresco	−0.01	2.19	1.26	0.88	3.10	1.40
	5rBF	Red	Buon Fresco	2.62	9.45	5.64	2.24	8.36	4.97
	9rBF	Red	Buon Fresco	3.75	6.17	4.05	2.56	4.55	3.34
	12rLF	Red	Lime Fresco	1.8	5.31	2.98	3.83	8.03	2.42
	5rLF	Red	Lime Fresco	1.68	7.29	4.12	1.15	5.70	3.00
	9rLF	Red	Lime Fresco	0.8	2.74	1.48	0.79	2.87	1.34
	1yBF	Yellow	Buon Fresco	−1.34	6.12	1.70	0.51	6.63	1.89
	5yBF	Yellow	Buon Fresco	−1.65	5.85	1.86	0.35	4.47	2.01
	9yBF	Yellow	Buon Fresco	−0.75	6.55	1.96	0.08	5.68	2.11
	3yLF	Yellow	Lime Fresco	0.85	3.40	1.06	0.58	2.78	0.90
	5yLF	Yellow	Lime Fresco	0.32	4.85	1.15	0.05	4.39	1.38
	9yLF	Yellow	Lime Fresco	0.69	8.12	2.51	0.69	8.29	2.57
	1bLF	Blue	Lime Fresco	2.38	2.69	0.47	2.44	2.63	0.51
	5bLF	Blue	Lime Fresco	1.32	1.34	0.01	0.93	1.03	0.15
	9bLF	Blue	Lime Fresco	0.68	0.79	0.22	−0.39	0.51	0.19
PrimalTM SF-016 ER®	2rBF	Red	Buon Fresco	−0.41	0.44	0.16	−0.35	0.99	0.18
	6rBF	Red	Buon Fresco	−0.15	1.48	0.18	−0.93	1.53	0.40
	10rBF	Red	Buon Fresco	0.14	0.34	0.02	0.15	0.93	0.43
	2rLF	Red	Lime Fresco	0.41	1.12	0.18	−0.24	2.11	0.57
	6rLF	Red	Lime Fresco	0.36	1.00	0.72	0.07	1.08	0.23
	10rLF	Red	Lime Fresco	0.18	0.36	0.05	−0.03	0.76	0.21
	2yBF	Yellow	Buon Fresco	−0.93	1.07	0.08	−1.03	1.12	0.003
	6yBF	Yellow	Buon Fresco	−0.37	2.64	0.40	−0.88	3.42	0.49
	10yBF	Yellow	Buon Fresco	0.45	0.46	0.10	−0.14	1.01	0.90
	2yLF	Yellow	Lime Fresco	−0.09	0.21	0.11	−1.07	1.28	0.30
	6yLF	Yellow	Lime Fresco	0.55	1.11	0.03	−0.7	1.64	0.11
	10yLF	Yellow	Lime Fresco	−0.71	1.40	0.41	−2.63	3.44	0.43
	2bLF	Blue	Lime Fresco	0.45	0.47	0.14	−0.21	0.22	0.06
	6bLF	Blue	Lime Fresco	0.52	0.52	0.64	1.01	1.01	0.03
	10bLF	Blue	Lime Fresco	−0.68	0.75	0.14	−0.51	0.53	0.09
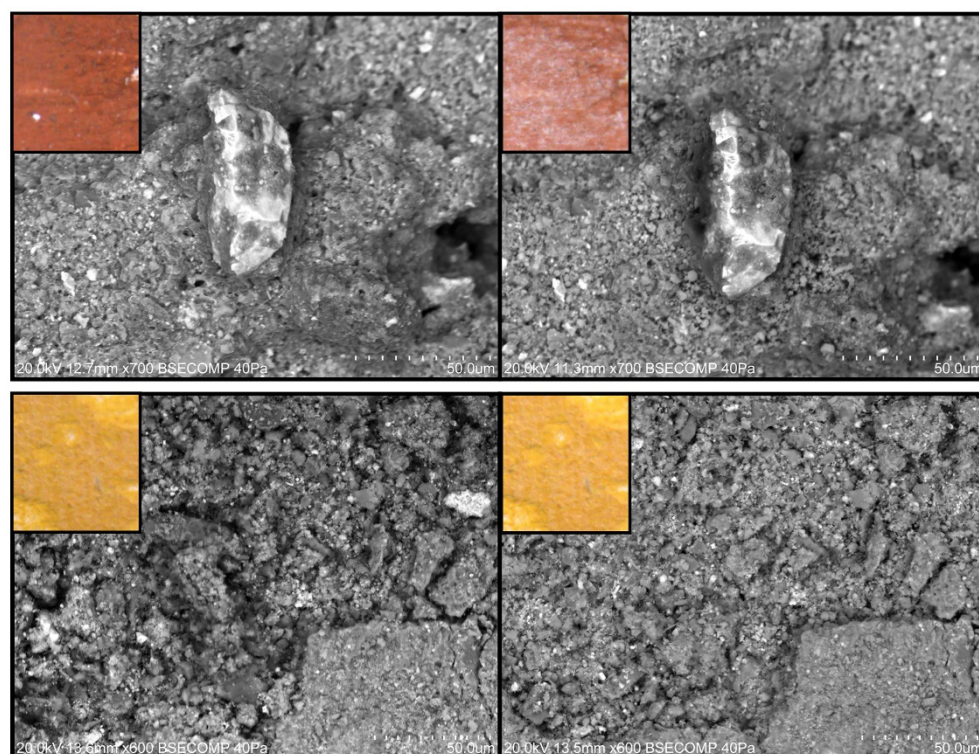
Figure A3. SEM images of red and yellow paint layers treated with LAB nanolime; before and one week after treatment: **Upper** image: rLF; **Lower** image: yBF. Detail images obtained by OM-Vis of the studied areas are in the top left corner.

References

1. ICOMOS. Principios Para la Preservación, Conservación y Restauración de Pinturas Murales. In Proceedings of the 14ª Asamblea General del ICOMOS, Victoria Falls, Zimbabwe, 27–31 October 2003.
2. Mora, P.; Mora, L.; Philipott, P. *Conservation of Wall Paintings*; Butterwoths: Oxford, UK, 1984.
3. Fichner-Rathus, L. *Understanding Art*, 10th ed.; Wadsworth: Boston, MA, USA, 2013; ISBN 13-978-1-111-83695-5.
4. Mora, P. *Causes of Deterioration of Mural Paintings*; International Centre for the Study of the Preservation and Restoration of Cultural Property (ICCROM): Rome, Italy, 2018.
5. Spencer, B.N.; Rosenthal, A.; Podany, J.; Larson, J.H.; Zaccari, F. Art Conservation and Restoration, Encyclopaedia Britannica. Available online: https://www.britannica.com/art/art-conservation-and-restoration (accessed on 1 November 2020).
6. Gil, M. *Conservação de Pintura Mural, Estudo e Consolidação de Argamassas de Cal Aérea e Areia com Falta de Coesão*; Laboratório Nacional de Engenharia Civil: Lisboa, Portugal, 2002.
7. Magaloni, K.D. La pintura mural y su conservación. *Arqueol. Mex.* **2011**, *108*, 33–37.
8. Rodrigues, J.D. Consolidation of decayed stones. A delicate problem with few practical solutions. In Proceedings of the 3rd International Seminar, Guimarães, Portugal, 7–9 November 2001; pp. 3–14.
9. Zhu, J.; Zhang, P.; Ding, J.; Dong, Y.; Cao, Y.; Dong, W.; Zhao, X.; Li, X.; Camaiti, M. Nano Ca(OH)2: A review on synthesis, properties and applications. *J. Cult. Herit.* **2021**, *50*, 25–42. [CrossRef]
10. Brajer, I.; Kalsbeek, N. Limewater Absorption and Calcite Crystal Formation on a Limewater-Impregnated Secco Wall Painting. *Stud. Conserv.* **1999**, *44*, 145–156. [CrossRef]
11. Baglioni, P.; Chelazzi, D.; Giorgi, R. *Nanotechnologies in the Conservation of Cultural Heritage, a Compendium of Materials and Techniques*; Springer: Heidelberg, Germany, 2015. [CrossRef]
12. Kaszowska, Z.; Kot, M.; Białek-Kostecka, D.; Forczek-Sajdak, A. Application of micro-indentation tests to assess the consolidation procedure of historic wall paintings. *J. Cult. Herit.* **2018**, *36*, 286–296. [CrossRef]
13. Normand, L.; Duchêne, S.; Vergès-Belmin, V.; Dandrel, C.; Giovannacci, D.; Nowik, W. Comparative in Situ Study of Nanolime, Ethyl Silicate and Acrylic Resin for Consolidation of Wall Paintings with High Water and Salt Contents at the Chapter Hall of Chartres Cathedral. *Int. J. Arch. Herit.* **2020**, *14*, 1120–1133. [CrossRef]
14. Baglioni, P.; Carretti, E.; Dei, L.; Giorgi, R. Nanotechnology in wall painting conservation. In *Self-Assembly*; Robinson, B.H., Ed.; IOS-Press: Amsterdam, The Netherlands, 2013; pp. 32–41. ISBN 1-58603-382-4.
15. Girginova, P.I.; Galacho, C.; Veiga, R.; Silva, A.S.; Candeias, A. Inorganic Nanomaterials for Restoration of Cultural Heritage: Synthesis Approaches towards Nanoconsolidants for Stone and Wall Paintings. *ChemSusChem* **2018**, *11*, 4168–4182. [CrossRef]

16. David, M.E.; Ion, R.-M.; Grigorescu, R.M.; Iancu, L.; Andrei, E.R. Nanomaterials Used in Conservation and Restoration of Cultural Heritage: An Up-to-Date Overview. *Materials* **2020**, *13*, 2064. [CrossRef]

17. Lisuzzo, L.; Cavallaro, G.; Milioto, S.; Lazzara, G. Halloysite nanotubes filled with MgO for paper reinforcement and deacidification. *Appl. Clay Sci.* **2021**, *213*, 106231. [CrossRef]

18. Rodriguez-Navarro, C.; Ruiz-Agudo, E. Nanolimes: From synthesis to application. *Pure Appl. Chem.* **2017**, *90*, 523–550. [CrossRef]

19. Becerra, J.; Zaderenko, A.P.; Ortiz, P. Basic Protocol for on-site testing consoli-dant nanoparticles on stone cultural heritage. *Heritage* **2019**, *2*, 2712–2724. [CrossRef]

20. Cavallaro, G.; Milioto, S.; Parisi, F.; Lazzara, G. Halloysite Nanotubes Loaded with Calcium Hydroxide: Alkaline Fillers for the Deacidification of Waterlogged Archeological Woods. *ACS Appl. Mater. Interfaces* **2018**, *10*, 27355–27364. [CrossRef]

21. Camerini, R.; Chelazzi, D.; Giorgi, R.; Baglioni, P. Hybrid nano-composites for the consolidation of earthen masonry. *J. Colloid Interface Sci.* **2018**, *539*, 504–515. [CrossRef]

22. Gómez-Villalba, L.S.; López-Arce, P.; Fort, R.; Álvarez, M. La aportación de la nanociencia a la conservación de bienes del patrimonio cultural. *Patrim. Cult. Esp.* **2010**, *4*, 43–56.

23. Girginova, P.I.; Galacho, C.; Veiga, R.; Silva, A.S.; Candeias, A. Study of mechanical properties of alkaline earth hydroxide nanoconsolidants for lime mortars. *Constr. Build. Mater.* **2019**, *236*, 117520. [CrossRef]

24. López-Arce, P.; Gómez-Villalba, L.; Martinez-Ramirez, S.; de Buergo, M.; Fort, R. Influence of relative humidity on the carbonation of calcium hydroxide nanoparticles and the formation of calcium carbonate polymorphs. *Powder Technol.* **2011**, *205*, 263–269. [CrossRef]

25. Álvarez, A.E.; Nadal, L.F. Evaluación del proceso de carbonatación de nanocales aplicadas a pinturas murales prehispánicas de origen maya. *Interv. Rev. Int. Conserv. Restauración Museol.* **2010**, *1*, 31–41. [CrossRef]

26. Vojtěchovský, J. Surface consolidation of wall paintings using lime nano-suspensions. *Acta Polytech.* **2017**, *57*, 139–148. [CrossRef]

27. Becherini, F.; Durante, C.; Bourguignon, E.; Vigni, M.L.; Detalle, V.; Bernardi, A.; Tomasin, P. Aesthetic compatibility assessment of consolidants for wall paintings by means of multivariate analysis of colorimetric data. *Chem. Cent. J.* **2018**, *12*, 98. [CrossRef]

28. Bourguignon, E.; Tomasin, P.; Detalle, V.; Vallet, J.-M.; Labouré, M.; Olteanu, I.; Favaro, M.; Chiurato, M.A.; Bernardi, A.; Becherini, F. Calcium alkoxides as alternative consolidants for wall paintings: Evaluation of their performance in laboratory and on site, on model and original samples, in comparison to conventional products. *J. Cult. Herit.* **2018**, *29*, 54–66. [CrossRef]

29. Ambrosi, M.; Dei, L.; Giorgi, R.; Neto, C.; Baglioni, P. Colloidal Particles of Ca(OH)2: Properties and Applications to Restoration of Frescoes. *Langmuir* **2001**, *17*, 4251–4255. [CrossRef]

30. Daehne, A.; Herm, C. Calcium hydroxide nanosols for the consolidation of porous building materials-results from EU-STONECORE. *Herit. Sci.* **2013**, *1*, 11. [CrossRef]

31. Baglioni, P.; Chelazzi, D.; Giorgi, R.; Carretti, E.; Toccafondi, N.; Jaidar, Y. Commercial Ca(OH)$_2$ nanoparticles for the consolidation of immovable works of art. *Appl. Phys. A* **2013**, *114*, 723–732. [CrossRef]

32. Natali, I.; Saladino, M.L.; Andriulo, F.; Martino, D.C.; Caponetti, E.; Carretti, E.; Dei, L. Consolidation and protection by nanolime: Recent advances for the conservation of the graffiti, Carceri dello Steri Palermo and of the 18th century lunettes, SS. Giuda e Simone Cloister, Corniola (Empoli). *J. Cult. Herit.* **2014**, *15*, 151–158. [CrossRef]

33. Giorgi, R.; Bozzi, C.; Dei, L.; Gabbiani, C.; Ninham, A.B.W.; Baglioni, P. Nanoparticles of Mg(OH)2: Synthesis and Application to Paper Conservation. *Langmuir* **2005**, *21*, 8495–8501. [CrossRef]

34. Girginova, P.I.; Galacho, C.; Mirão, J.; Veiga, R.; Silva, A.S.; Candeias, A. Preliminary studies of consolidation of wall paintings: Synthesis and characterisation of nanolime. *Conserv. Património* **2016**, *23*, 103–107. [CrossRef]

35. Gil, M.; Rosado, T.; Ribeiro, I.; Pestana, J.A.; Caldeira, A.T.; Carvalho, M.L.; Dias, L.; Mirão, J.; Candeias, A. Are theyfrescopaintings? Technical and material study ofCasas Pintadasof Vasco da Gama house in Évora (Southern Portugal). *X-Ray Spectrom.* **2015**, *44*, 154–162. [CrossRef]

36. Johnston-Feller, R. Color science in the examination of museum objects: Nondestructive procedures. *Color Res. Appl.* **2002**, *27*, 456–457. [CrossRef]

37. Michalopoulou, A.; Maravelaki, P.-N.; Kilikoglou, V.; Karatasios, I. Morphological characterization of water-based nanolime dispersions. *J. Cult. Herit.* **2020**, *46*, 11–20. [CrossRef]

38. Nasrazadani, S.; Eureste, E. Application of FTIR for Quantitive Lime Analysis. Available online: https://library.ctr.utexas.edu/digitized/texasarchive/phase2/9028-01-1.pdf (accessed on 1 December 2000).

39. Kimura, N.; Umemura, J.; Hayashi, S. Polarized FT-IR Spectra of Water in the Middle Phase of Triton X100-Water System. *J. Colloid Interface Sci.* **1996**, *182*, 356–364. [CrossRef]

40. Rajisha, K.R.; Deepa, B.; Pothan, L.A.; Thomas, S. Thermochemical and spectroscopic characterization of natural fibre composites. In *Interface Engineering of Natural Fibre Composites for Maximum Performance*; Zafeiropoulos, N.E., Ed.; Woodhead Publishing: Cambridge, UK, 2011; pp. 241–274.

41. Rodriguez-Navarro, C.; Suzuki, M.A.; Ruiz-Agudo, E. Alcohol Dispersions of Calcium Hydroxide Nanoparticles for Stone Conservation. *Langmuir* **2013**, *29*, 11457–11470. [CrossRef] [PubMed]

42. Delgado, J.R.; Grossi, A. Indicators and ratings for the compatibility assessment of conservation actions. *J. Cult. Herit.* **2007**, *8*, 32–43. [CrossRef]

43. Becerra, J.; Zaderenko, A.; Ortiz, R.; Karapanagiotis, I.; Ortiz, P. Comparison of the performance of a novel nanolime doped with ZnO quantum dots with common consolidants for historical carbonate stone buildings. *Appl. Clay Sci.* **2020**, *195*, 105732. [CrossRef]

44. Borsoi, G.; Lubelli, B.; van Hees, R.; Veiga, R.; Silva, A.S.; Colla, L.; Fedele, L.; Tomasin, P. Effect of solvent on nanolime transport within limestone: How to improve in-depth deposition. *Colloids Surf. A Physicochem. Eng. Asp.* **2016**, *497*, 171–181. [CrossRef]

45. Lanzón, M.; De Stefano, V.; Gaitán, J.C.M.; Cardiel, I.B.; Gutiérrez-Carrillo, M.L. Characterisation of earthen walls in the Generalife (Alhambra): Microstructural and physical changes induced by deposition of Ca(OH)2 nanoparticles in original and reconstructed samples. *Constr. Build. Mater.* **2019**, *232*, 117202. [CrossRef]

46. Ševčík, R.; Mácová, P.; Estébanez, M.P.; Viani, A. Influence of additions of synthetic anhydrous calcium carbonate polymorphs on nanolime carbonation. *Constr. Build. Mater.* **2019**, *228*, 116802. [CrossRef]

47. Gherardi, F.; Otero, J.; Blakeley, R.; Colston, B. Application of Nanolimes for the Consolidation of Limestone from the Medieval Bishop's Palace, Lincoln, UK. *Stud. Conserv.* **2020**, *65*, P90–P97. [CrossRef]

48. Dei, L.; Salvadori, B. Nanotechnology in cultural heritage conservation: Nanometric slaked lime saves architectonic and artistic surfaces from decay. *J. Cult. Herit.* **2006**, *7*, 110–115. [CrossRef]

49. López-Martínez, T.; Otero, J. Preventing the Undesired Surface Veiling after Nanolime Treatments on Wall Paintings: Preliminary Investigations. *Coatings* **2021**, *11*, 1083. [CrossRef]